chromosome 19q13.3 (DM protein kinase gene with cytosine–thymine–guanine (CTG) repeats expansion) (DM-1), and in chromosome 3q21 (*ZNF9* gene with cytosine–cytosine–thymine–guanine (CCTG) repeats expansion) (DM-2). The third gene is linked to chromosome 15q21–24 (DM-3). In these cases of DM, microvacuolar and macrovacuolar spogiform degeneration have been observed in frontal, temporal and insular corticies. But tau inclusions are rare, and no amyloid deposit has been found in cases of DM-3.

The recent findings in neuropathological and genetic research have been summarized above. As indicated, further investigation of the roles of tau, neurofilaments, PS and VCP in the cellular process of neurodegeneration is necessary to understand the molecular pathogenesis of the neurodegenerative disorders described previously. As has been shown, FTD has many variations and subgroups, and one of the clinically important aspects of FTD is the management of behavioral and psychiatric symptoms of dementia (BPSD). The problem-solving approach for the management of BPSD is based on the administration of appropriate medicine and sufficient understanding of symptoms by caregivers. FTD has several variations in symptoms, and the regional pattern of neurodegeneration, rather than the type of histopathology, influences the clinical syndrome in FTD.[11] Brain imaging analysis is also important for understanding the regions of the brain that are impaired. Therefore, advances in our knowledge of biochemical and/or genetic causes of FTD may lead to a more accurate and appropriate reclassification of FTD for future pharmaceutical therapeutics, and current brain imaging analysis may provide important information for understanding the pathogenesis of clinical symptoms.

REFERENCES

1 Cairns NJ, Perry RH, Jaros E *et al.* Patients with a novel neurofilamantopathy: dementia with neurofilament inclusions. *Neurosci Lett* 2003; **341**: 177–180.

2 Cairns NJ, Zhukareva V, Uryu K *et al.* Alpha-internexin is present in the pathological inclusions of neuronal intermediate filament inclusion disease. *Am J Pathol* 2004; **164**: 2153–2161.

3 Cairns NJ, Grossman M, Arnold SE *et al.* Clinical and neuropathologic variation in neuronal intermediate filament inclusion disease. *Neurology* 2004; **63**: 1376–1384.

4 Hutton M, Lendon CL, Rizzu P *et al.* Association of missense and 5′-splice-site mutations in tau with the inherited dementia FTDP-17. *Nature* 1998; **393**: 702–705.

5 Dermaut B, Kumar-Singh S, Engelborghs S *et al.* A novel presenilin-1 mutation associated with Pick's disease but not beta-amyloid plaques. *Ann Neurol* 2004; **55**: 617–626.

6 Halliday GM, Song YJ, Lepar G *et al.* Pick bodies in a family with presenilin-1 Alzheimer's disease. *Ann Neurol* 2005; **57**: 139–143.

7 Amtul Z, Lewis PA, Piper S *et al.* A presenilin-1 mutation associated with familial frontotemporal dementia inhibits gamma-secretase cleavage of APP and notch. *Neurobiol Dis* 2002; **9**: 269–273.

8 Watts GD, Wymer J, Kovach MJ *et al.* Inclusion body myopathy associated with Paget disease of bone and frontotemporal dementia is caused by mutant valosin-containing protein. *Nat Genet* 2004; **36**: 377–381.

9 Yancopoulou D, Crowther RA, Chakrabarti L *et al.* Tau protein in frontotemporal dementia linked to chromosome 3 (FTD-3). *J Neuropathol Exp Neurol* 2003; **62**: 878–882.

10 Le Ber I, Martinez M, Campion D *et al.* A non-DM1, non-DM2 multisystem myotonic disorder with frontotemporal dementia: phenotype and suggestive mapping of the DM3 locus to chromosome 15q21–24. *Brain* 2004; **127**: 1979–1992.

11 Kril JJ, Macdonald V, Patel S *et al.* Distribution of brain atrophy in behavioral variant frontotemporal dementia. *J Neurol Sci* 2005; **232**: 83–90.

Available online at www.sciencedirect.com
SCIENCE DIRECT
Brain Research 1040 (2005) 73–80
BRAIN RESEARCH
www.elsevier.com/locate/brainres

Research report

α-Synuclein-positive structures induced in leupeptin-infused rats

T. Nakajima[a,*], S. Takauchi[b], K. Ohara[a], M. Kokai[a], R. Nishii[a], S. Maeda[c], A. Takanaga[c], T. Tanaka[d], M. Takeda[d], M. Seki[c], Y. Morita[a]

[a]*Department of Neuropsychiatry, Hyogo College of Medicine, 1-1 Mukogawa-cho, Nishinomiya, Hyogo 663-8501, Japan*
[b]*Faculty of Health and Welfare, Osaka University of Health and Sport Science, 1-1 Asashirodai, Kumatori-cho, Sennan, Osaka 590-0459, Japan*
[c]*Department of 1st Anatomy, Hyogo College of Medicine, 1-1 Mukogawa-cho, Nishinomiya, Hyogo 663-8501, Japan*
[d]*Division of Psychiatry and Behavioral Proteomics, Department of Post-Genomics and Diseases, Course of Advanced Medicine, Osaka University, Graduate School of Medicine, D-3, 2-2 Yamadaoka, Suita, Osaka 565-0871, Japan.*

Accepted 21 January 2005
Available online 11 March 2005

Abstract

Abnormal accumulation of α-synuclein is regarded as a key pathological step in a wide range of neurodegenerative processes, not only in Parkinson's disease (PD) and dementia with Lewy bodies (DLB) but also in multiple-system atrophy (MSA). Nevertheless, the mechanism of α-synuclein accumulation remains unclear. Leupeptin, a protease inhibitor, has been known to cause various neuropathological changes in vivo resembling those of aging or neurodegenerative processes in the human brain, including the accumulation of neuronal processes and neuronal cytoskeletal abnormalities leading to neurofibrillary tangle (NFT)-like formations. In the present study, we administered leupeptin into the rat ventricle and found that α-synuclein-positive structures appeared widely in the neuronal tissue, mainly in neuronal processes of the fimbria and alveus. Immunoelectron microscopic study revealed that α-synuclein immunoreactivity was located in the swollen axons of the fimbria and alveus, especially in the dilated presynaptic terminals. In addition colocalization of α-synuclein with ubiquitin was rarely observed in confocal laser-scan image. This is the first report of experimentally induced in vivo accumulation of α-synuclein in non-transgenic rodent brain injected with a well-characterized protease inhibitor by an infusion pump. The present finding suggests that the local accumulation of α-synuclein might be induced by the impaired metabolism of α-synuclein, which are likely related to lysosomal or ubiquitin-independent proteasomal systems.

Theme: Disorders of the nervous system
Topic: Degenerative disease: Parkinson's

Keywords: α-Synuclein; Leupeptin; Protease inhibitor; Immunohistochemistry; Immunoelectron microscopy

1. Introduction

Lewy bodies (LB) and Lewy neurites are universally recognized as pathological hallmarks of Parkinson's disease (PD) and dementia with Lewy bodies (DLB). Although LB can be observed microscopically with hematoxylin-eosin stain, an immunohistochemical method for detection of LB with either anti-ubiquitin or anti-α-synuclein antibody is recommended [1,6]. α-Synuclein has been proven to be one of the major components of LB in PD and DLB [9,26]; however, aggregation of α-synuclein is also demonstrated in the brains of Alzheimer's disease (AD) patients [17]. In addition, two recent cases of patients with diffuse neurofibrillary tangles disease with calcification (DNTC) have shown that neurons containing α-synuclein-positive structures are widely distributed, especially in the amygdala, hippocampus, and upper temporal gyrus [32]. Because the pure form of DLB, that is, DLB without or with very few neurofibrillary tangles or senile plaques is known [13], the process of Lewy body formation would not comprise a simple linkage of NFT formations. On the contrary, the frequent coexistence of NFT and LB in AD brains indicated that there may be a relationship between the mechanism of tau

* Corresponding author. Fax: +81 798 45 6053.
E-mail address: taka528i@kcc.zaq.ne.jp (T. Nakajima).

0006-8993/$ - see front matter © 2005 Elsevier B.V. All rights reserved.
doi:10.1016/j.brainres.2005.01.099

accumulation and that of α-synuclein accumulation in the AD and DNTC brains, although these mechanisms are so far unknown.

Leupeptin, a protease inhibitor, is known to cause (1) the accumulation of lipofuscin-like granules in the neuronal perikarya and (2) the degeneration of neurites [4,7,27]. Furthermore, we previously reported that the long-term infusion of leupeptin into the rat ventricle caused cytoskeletal changes that included the formation of abnormal bundles of paired helical filament-like filaments with 20 nm diameter and periodic constrictions at 40 nm intervals in the cortical neuron [28]. We reported that these changes had some morphological resemblance to neuropathological features of Alzheimer's brains.

In the present study, we found, by the administration of leupeptin to the rat brain, that α-synuclein-positive structures appeared in various portions of the brain in response to the degeneration caused by leupeptin. Immunoelectron microscopic studies revealed that α-synuclein-positive materials accumulated in the swollen axons, especially in dilated presynaptic terminals and in the neuronal cell bodies. These results revealed that a disturbance of protein degradation causes not only cytoskeletal abnormality, as we reported before, but also α-synuclein accumulation in the neurons. In this study, it suggests that impairment of protein degradation might be closely related with neurodegenerative diseases including AD that is characterized by cytoskeletal abnormality with accumulation of tau, amyloid β, and α-synuclein. It was reported that decreased activities of proteasome were observed in AD brain [12], and that in cultured cells protease-dysfunction induced neuronal degeneration [10]. Therefore, we would like to raise the hypothesis that disturbed protein-degradative activities are initial causative events leading to neurodegenerative disorders, even though the cause of dysfunction of protein degradation was not clarified. Recently, in the study of polyglutamine disease, one of neurodegeneration diseases, dysfunction of proteasome was found to be an initial event in the degenerative processes, and it might support our thought.

Previously accumulation of α-synuclein was reported in transgenic-model mouse [25,30], or rodents injected with MPTP or rotenone [3,5,16]. Both of chemical compounds were not well characterized in biochemical function on the mechanisms of cytotoxicity yet, even though oxidative stress mechanisms are thought to be mediators in either compound. This is the first report of experimentally induced in vivo accumulation of α-synuclein in non-transgenic rodent brain injected with leupeptin, a biochemically well-characterized protease inhibitor, by an infusion pump.

2. Materials and methods

Twenty 8-week-old Wistar rats, weighting about 300 g, were used for the present study. Leupeptin (Peptide Institute Inc., Osaka, Japan) solution, dissolved in phosphate-buffered saline (pH 7.4) at 25 mg/ml, was infused with an osmotic minipump (Model 2002; Alzet, California, USA). The outline of the operation was described elsewhere [27]. The pump was connected by means of a Silastic tube to an intracerebroventricular cannula and implanted subcutaneously in the neck. The cannula was implanted stereotaxically (0.8 mm posterior to the bregma, 1.2 mm lateral to the midline) into the right lateral ventricle. Five rats were implanted with pumps containing only phosphate-buffered saline (PBS) and served as controls.

2.1. Immunomicroscopy

Following infusion for 14 days, the rats were anesthetized and killed by perfusion through the left ventricle with 4% buffered paraformaldehyde solution.

For immunomicroscopic study, brains were dissected and fixed for 24 h in 4% paraformaldehyde in 0.1 M phosphate buffer (PB) (pH 7.4). The brains, including the brain stem and the spinal cord, were cut coronally at 3 mm thickness. The slices were rinsed with PB, dehydrated through graded alcohol, and embedded in paraffin. Paraffin sections at 10 μm were made, deparaffinated, and prepared for immunostaining. Immunostaining was performed with monoclonal anti-α-synuclein antibody synuclein-1 (1:500 dilution) (Transduction Laboratories, Lexington, USA) as the primary antibody [20]. Sections were incubated overnight at 4 °C. For the immunohistochemical detection of the primary antibody, sections were incubated with a secondary antibody (1:100 biotinylated anti-mouse; Vector Laboratories, Burlingame, USA) for 2 h at room temperature. After rinsing in PB, the sections were then incubated in avidin–biotin–peroxidase complex (Vector Laboratories, Burlingame, USA) for 1 h at room temperature. After three subsequent washings in PB, sections were visualized by diaminobenzidine tetrahydrochloride.

2.2. Immunoelectron microscopy

For immunoelectron microscopic study, the rats were perfused with 4% paraformaldehyde, 0.1% glutaraldehyde, and 15% picric acid in 0.1 M PB (pH 7.4). Brains were fixed for 24 h in 4% paraformaldehyde, 7% sucrose in PB. The leupeptin-treated rat brains were cut by vibratome to make 50-μm-thick coronal slices and there were washed in PB. Sections were first incubated overnight with the anti-α-synuclein antibody (1:500 dilution) at 4 °C, then incubated for 2 h with the secondary antibody (1:100 biotinylated anti-mouse; Vector Laboratories, Burlingame, USA), and treated with the avidin–biotin–peroxidase complex for 1 h at room temperature. After three subsequent washings in PB, sections were visualized by diaminobenzidine (DAB) tetrahydrochloride. For the post-fixation for electron microscopy, sections were incubated with 4% paraformaldehyde and 0.1% glutaraldehyde in PB

(pH 7.4) for 3 days. And then, sections were osmicated with 2% OsO4 in PB and dehydrated through graded alcohol.

DAB-development was rigorously performed for 10 min, and the slices were fixed with 2.5% glutaraldehyde and 4% paraformaldehyde in PB (pH 7.4). They were slightly washed and post-fixed with 2% OsO4 in PB for 1 h at 4 °C, then flatly embedded in Spurr's resin (TAAB, Berkshire, UK) between aclar films (Nissin EM, Tokyo, Japan). Polymerization was performed overnight at 70 °C, and the specimens were pre-examined by light microscopy. The areas including positive reactions in CA4 and fimbria were trimmed, and ultra-thin sections were made with an Ultracut UCT microtome (Leica, Solms, Germany) and examined by transmission electron microscopy with a JEM 1200 EX (JEOL, Tokyo, Japan) at 80 kV.

2.3. SDS–PAGE and Western blotting

Respectively five leupeptin-infused rats and control rats were used to study the expression of α-synuclein in fimbria. Operated rats were deeply anesthetized with diethyl ether and killed by decapitation. Their brains were removed and immediately washed with ice-cold PBS. Hippocampi of the right cerebra were dissected and the fimbriae were removed. The frontal quarter of the fimbriae were cut and immersed for 3 h in 4% paraformaldehyde, 7% sucrose in PB, for overnight 20% sucrose in PB to study confocal laser-scanning microscopy. Three quarters of the remaining fimbriae were homogenized in 0.05 M Tris–HCl (pH 7.4) containing 0.1% Triton X-100 with a Potter type glass-Teflon homogenizer. Specimens were gently centrifuged (at 900 × *g* for 5 min) to remove the debris and the proteins were precipitated by the addition of 9 volumes of cold methanol. They were centrifuged at 10.000 × *g* for 10 min and re-suspended in deionized water. The protein concentrations of each extract were determined by using a spectrometer Smart Spec™ 3000 (Bio Rad, USA) and adjusted to 1 mg/ml with 0.05 M Tris–HCl buffer (pH 7.4). The samples were denatured with Laemmli's sample buffer (Laemmli, 1970), carried out SDS–PAGE in a 15% acrylamide gel, and transferred to a polyvinylidene difluoride membrane (Boehringer Mannheim, Germany). The membrane was blocked with Block Ace™ for 1 h, and then incubated with anti α-synuclein antibody and mouse anti α-tubulin (Oncogene, USA), as an internal standard, for 2 h at room temperature. After washing, the membrane was incubated with HRP-conjugated goat anti-mouse IgG (Vector Labs, USA) for 2 h at room temperature. The signal was detected by using chemiluminescent detection system (ECL™ + Plus, Amersham Pharmacia Biotech, UK) and visualized by exposure on X-ray film (Fuji Photo Film, Japan). The signal intensities were quantified using densitometric analysis by Scion Image program (Scion Co., NIH, USA), and compared by student *t* test ($P < 0.05$).

2.4. Confocal laser-scanning microscopy

The frozen frontal quarter of the fimbriae was cut by cryostat to make 20-μm-thick slices. These sections were simultaneously incubated for 3 days with mouse anti-α-synuclein monoclonal antibody synuclein-1 (1:4000 dilution) (Transduction Laboratories, Lexington, USA) and rabbit anti-ubiquitin polyclonal antibody (1:4000 dilution) (Chemicon, USA) at 4 °C, then simultaneously incubated for 2 h with Alexa Fluor 488 donkey anti mouse IgG (1:1000 dilution) (Morecular Probes, USA) and Cy™3-conjugated donkey anti rabbit IgG (1:1000 dilution) (Jackson ImmunoResearch, USA) at room temperature. A Zeiss confocal laser-scanning microscope (LSM510, Carl Zeiss, Germany) was used to visualize the fluorescent materials. By scanning simultaneously with two lasers (488 and 543 nm) and by using ×20 objective, we obtained a two-color image of the fimbriae.

3. Results

3.1. Immunomicroscopic findings

α-Synuclein-positive structures appeared as evenly stained sporadic granules or spheroids with clear contours. They were distributed in the alveus (Fig. 1c), fimbria (Fig. 1d), as well as in the external capsule and the deep layer of the cerebral cortex on the infused side of the leupeptin-treated rats. Qualitatively the α-synuclein structures appear to be abundant in the alveus and fimbria. Furthermore, they appear to be numerous in the external capsule than in the deep layer of the cerebral cortex (data not shown). From the present observation and our previous electron microscopic study [28], these α-synuclein-positive structures seem to correspond to the degenerated axons originating from pyramidal cells in the hippocampus.

In contrast, no α-synuclein-positive structure was observed in other regions of the central nervous system (CNS) of leupeptin-treated rats (Figs. 1e and f) or in the whole CNS of control rats (Figs. 1a and b). To evaluate specificity of the antibody, the staining procedure without application of the primary antibody was performed, and only background staining was observed in leupeptin-treated (Figs. 1g and h) and leupeptin-non-treated rat (data not shown).

3.2. Immunoelectron microscopic findings

The accumulation of dense bodies in the neuronal perikarya and in the swollen neuronal processes, which we had previously reported, was also detected in the specimens for the present experiment.

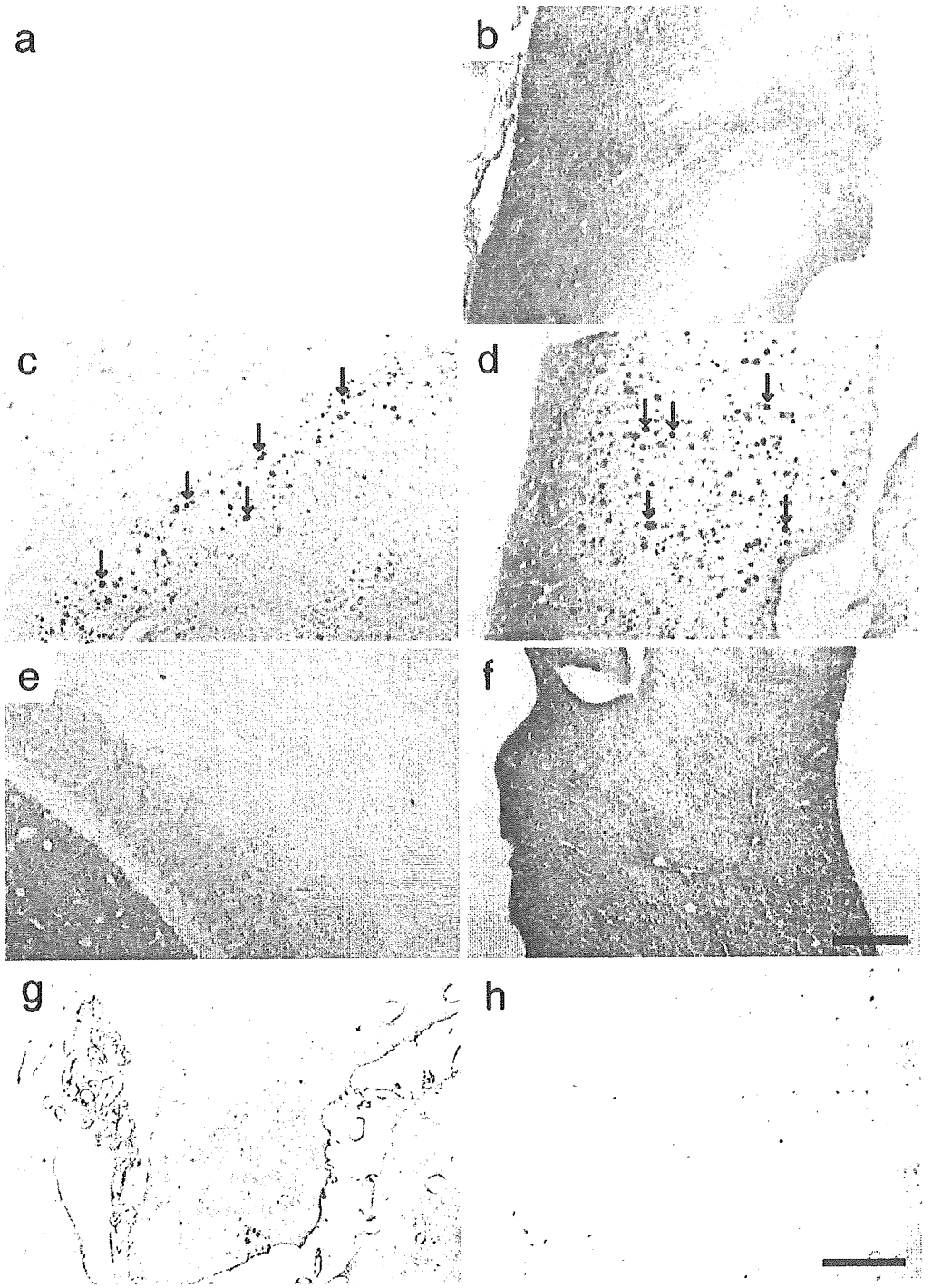

Fig. 1. (a–h) Immunohistochemical staining in rat fimbria and alveus. (a and b) Immunohistochemical staining of α-synuclein in control rat brain hippocampus. No α-synuclein-positive structure was observed in alveus (a), and fimbria (b). (c–f) Immunohistochemical staining of α-synuclein in leupeptin-treated rat brain hippocampus. (c and d) Leupeptin infused side. (e and f) Leupeptin non-infused side. α-Synuclein-positive structures (arrows) were observed in alveus (c) and fimbria (d) of the infused side. No α-synuclein-positive structures were observed in the corresponding areas of the non-infused side (e and f) (scale bar = 100 μm). (g and h) Immunohistochemical staining without primary antibody (scale bar = 200 μm).

Anti-α-synuclein immunoreactivity was found exclusively in the neuronal component of the leupeptin-treated rats, mainly in swollen axons of the fimbria and alveus of the hippocampus (Fig. 2a). The immunoreactivity appeared as small granules or more fuzzy electron-dense material filling the spaces among accumulated mitochondria and dense bodies observed in the so-called degenerated neurites (Fig. 2b).

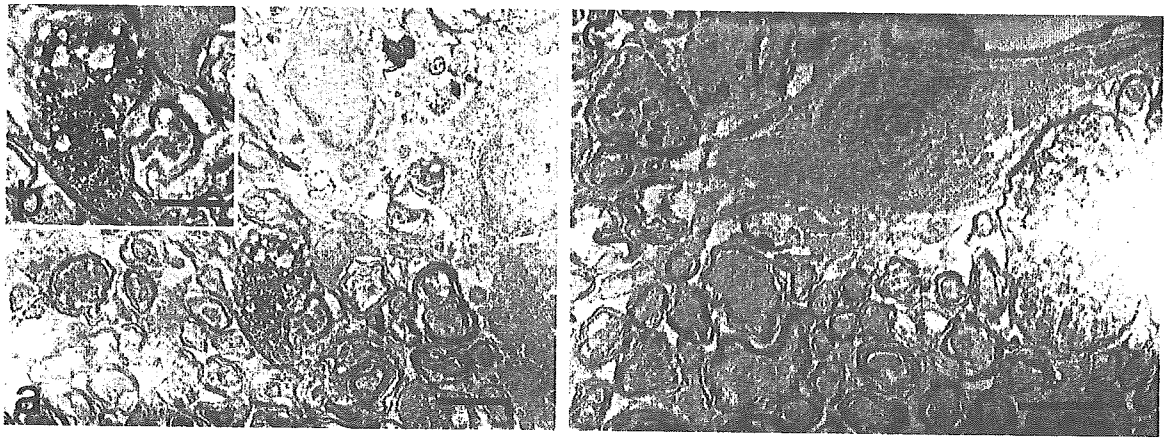

Fig. 2. (a and b) Immunoelectron microscopy for α-synuclein in leupeptin infused rat brain hippocampus. (a) A transverse section of a swollen axon in the fimbria (SP*) (scale bar = 2 μm). (b) A higher resolution immunoelectron micrograph of a swollen axon in the fimbria (scale bar = 1 μm). (c) Control rat brain hippocampus (scale bar = 2 μm).

3.3. SDS–PAGE and Western blottings

Western blot analysis showed a 19-kDa α-synuclein band in both the leupeptin-infused and the control rat hippocampal extracts (Fig. 3a); however, the densities of these reactions were obviously different. No band with higher molecular weight was observed in both experimental and control rats (Fig. 3a). This finding suggests that accumulation of monomer forms of α-synuclein was induced by leupeptin. The densities of these bands were quantified by Scion Image software (Fig. 3b). The integrated density of the leupeptin-infused specimens was 0.606 ± 0.08, and that of the control specimens was 0.421 ± 0.14. This indicates that the α-synuclein concentration in fimbria of the leupeptin-infused rats is significantly higher ($P < 0.05$) than that of the control rats.

3.4. Confocal laser-scanning microscopic findings

In the control rat fimbria (Figs. 4a–c), α-synuclein-positive structures (green) and ubiquitin-positive structures (red) were observed as diffusely distributed small granules. In the leupeptin-treated rat fimbria (Figs. 4d–f), α-synuclein-positive structures and ubiquitin-positive structures were observed as various sized and amorphous structures, and some cells were strongly labeled with anti-synuclein antibody only (arrows), or with anti-ubiquitin antibody only (arrowheads). In the merged images, colocalization of α-synuclein with ubiquitin was rarely observed.

4. Discussion

α-Synuclein, which is one of the presynaptic proteins, is composed of 140 amino acids [8] and is known to be identical to precursor (NACP) of the non-Aβ component of AD amyloid (NAC) [9]. The accumulation of α-synuclein has been demonstrated in Lewy bodies appearing in PD and DLB [1,6,26], as well as in degenerated neurons in the frontal lobe of AD [2]. In contrast to AD, in cases with multiple-system atrophy (MSA), these immunoreactivities were detected predominantly in glial cytoplasmic inclusions [31]. Moreover, neurons containing α-synuclein immunoreactive structures have been reported to be widely distributed in the amygdala, hippocampus, and superior temporal gyrus in DNTC [32]. These findings on the neurodegenerative process in general suggest that overproduction and disturbance of degradation of α-synuclein might play important roles in neuronal degeneration.

In the present experiment, leupeptin, a potent thiol protease inhibitor, was infused into the rat lateral ventricle. For two decades, leupeptin has been known to inhibit cathepsins and neural calcium-dependent protease and to cause various neuronal changes similar to those seen in the aging process or neuronal degeneration. By using the same experimental model, we have reported the accumulation of lipofuscin-like dense granules in the neuronal cell bodies, widespread degeneration of neuronal processes in the neuropil of the rat cerebral cortex, and formation of intraneuronal inclusions consisting of abnormal fibrillar structures, and we proposed that disturbances of protein turnover induced by leupeptin may have some pathogenic mechanisms in common with neuronal degeneration [27]. In this study we focus on α-synuclein. On the normal distribution of α-synuclein, the highest concentrations of α-synuclein mRNA are in the substantia nigra, the dentate granule cells and CA3 regions of the hippocampal formation, and the deep layers of the cortex [21]. Our immunohistochemical analysis in normal control revealed no obvious staining in DAB staining and dotlike structures in fluorescent staining. In the leupeptin-treated rat, immunolabeling of α-synuclein was observed in the neuropil of the fimbria, alveus. In stained neuronal cell bodies, the intense staining was distributed in whole cells, not as small punctate structures. Ultrastructurally, in normal rat brain, α-synuclein was present in synaptic boutons; however, in the leupeptin-

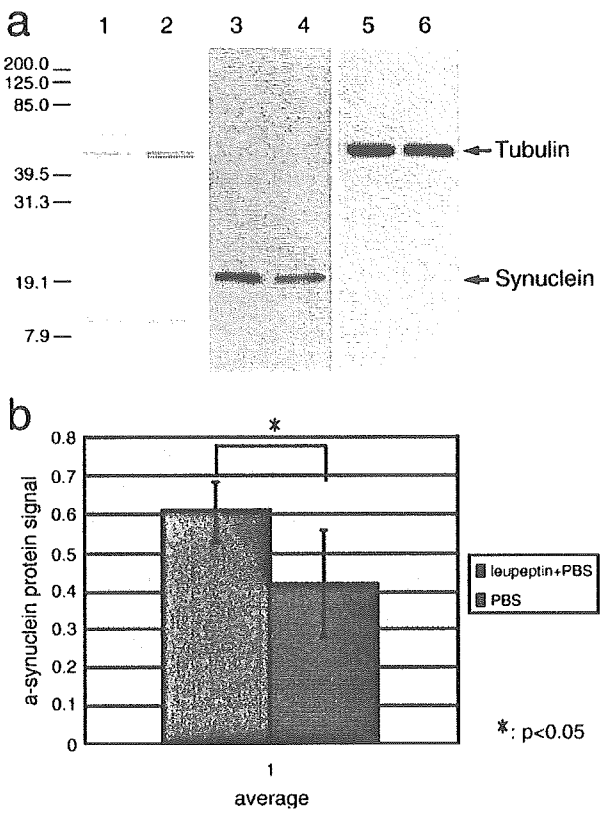

Fig. 3. (a and b) Western blotting analysis shows an increase of α-synuclein in leupeptin-infused rat fimbria. (a) Western blot analysis of α-synuclein shows an increase of α-synuclein in leupeptin-infused (lanes 1, 3, and 5) rat fimbria compared with PBS-infused (lanes 2, 4, and 6) rat fimbria. Total protein stained with Coomassie blue (lanes 1 and 2) and α-tubulin used as internal standard (lanes 5 and 6) indicates the same amount of applied sample proteins. A band of α-synuclein is detected in both leupeptin- and PBS-infused rats (lanes 3 and 4); however, the reaction density of the antibody is much more intense in lane 3 than in lane 4. Results are representative of five similar experiments. The numbers on the left indicate the molecular weight markers. The presented Western blot represents a typical result from one control and one leupeptin-treated rat brain. (b) Densitometric analysis of the Western blot is expressed as mean ± SD from five sets of experiments (*$P < 0.05$).

treated rat brain, α-synuclein immunoreactivity was observed especially in the swollen axons in the fimbria and alveus, and in the enlarged presynaptic axon terminals as fine granules filling the spaces among the dense bodies and other organelle.

Western blot analysis showed a 19-kDa α-synuclein bands in both of the hippocampal extracts from leupeptin-infused and the control rat; however, the intensities of these bands were obviously different. No other band with higher molecular weight was observed. Scion Image software revealed that the intensity of the band in the leupeptin-infused rats was significantly stronger than that of control rats. This finding suggests that accumulation of monomer forms of α-synuclein proteins was induced by leupeptin in the neuronal cell body by the infusion of leupeptin and this event might be a trigger to the formation of α-syn accumulation previously described in this model.

In confocal laser-scan imaging, both of the α-synuclein-positive labeling and the ubiquitin-positive labeling were visualized in cell bodies in leupeptin-treated rats, while they were visualized as dotlike structures in cells in control rats. In the merged images of double labeling, colocalization of α-synuclein with ubiquitin was rarely observed. These findings suggest that α-synuclein accumulation might not be related with ubiquitin-proteasome pathway. It is possible that α-synuclein accumulation might be caused by lysosome or ubiquitin-independent proteasome [29]. Leupeptin is known lysosomal protease inhibitor; however, biochemical study previously showed that leupeptin binds not only with lysosomal proteases, but also with the non-lysosomal degradation system protease, namely the proteasome [24], suggesting that it might affect the proteosome activity, even though inhibitory effects of leupeptin to proteasome were not confirmed yet [19]. In this study, ubiquitin-positive labeling seemed to be accumulated as well as α-synuclein-positive labeling in the fimbria in confocal laser scanning. This finding suggests that leupeptin, an inhibitor to several kinds of proteases, can affect metabolic processes of neuronal proteins, and that α-synuclein and ubiquitin might be influenced with different process by leupeptin, as the α-synuclein-positive labeling and ubiquitin-positive labeling were not co-localized.

As we did not find any fibrillar structures that are the usual components of typical Lewy bodies, the accumulation of α-synuclein cannot be directly connected with the mechanism of Lewy body formation. In addition, it remains unclear whether a disturbance of degradation of α-synuclein is one of the early steps in the generation of Lewy bodies prior to nitration or other modification of α-synuclein, or not. To clarify these questions, further experiments are required.

Normal α-synuclein immunoreactivity often forms deposits or small granules, but not fibrous structures. Lewy bodies from postmortem PD brains are largely composed of the insoluble form of α-synuclein which has fibrous structures. Misfolded or damaged proteins are potentially toxic and are generally degraded in an ubiquitin-dependent manner by the proteasome, Lewy bodies are ubiquitin-positive structures and α-synuclein, one of its component, is reported to be degraded by proteasome [2]. Several studies have suggested a link between ubiquitin-proteasome proteolysis system malfunction and an increase in ubiquitinated complexes [11,23]. α-Synuclein was aggregated and formed fibrous structures, when it accumulates up to a certain concentration [15,16]. Therefore at this moment the most plausible hypothesis on the pathological pathway is that down-regulated proteolysis causes increased α-synuclein and other misfolded or damaged proteins, and that completely insoluble forms α-synuclein attenuate ubiquitin-proteasome proteolysis sys-

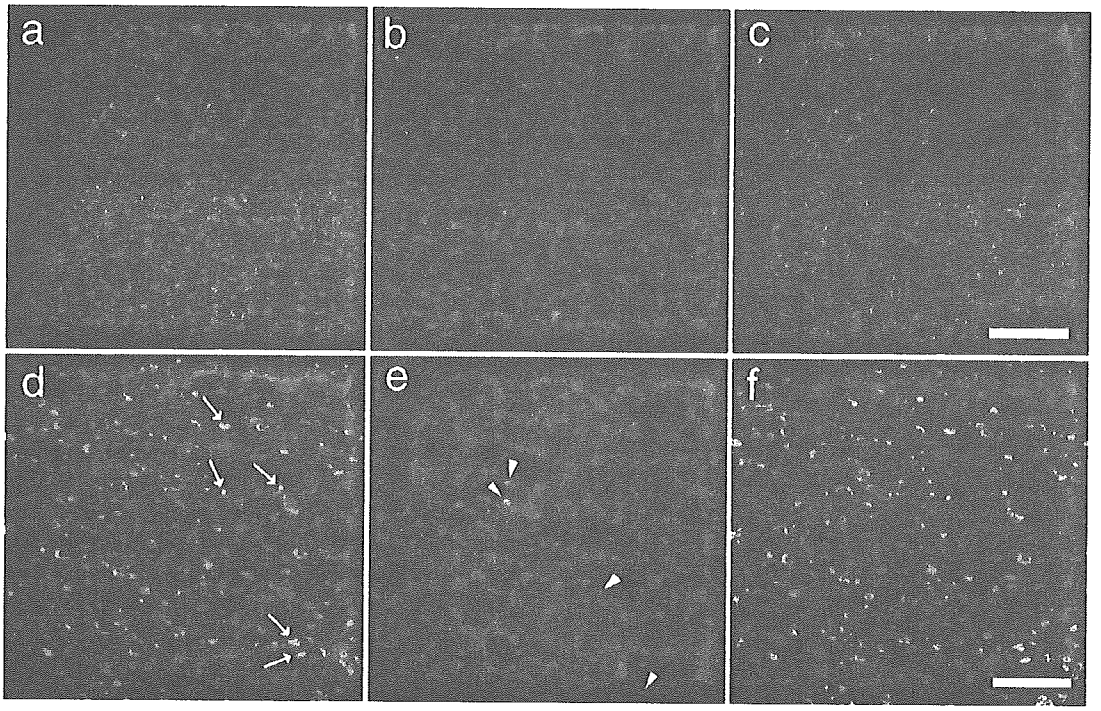

Fig. 4. (a–f) Confocal scanning images of the fimbria of rats at anti-α-synuclein (a and d; green), the anti-ubiquitin (b and e; red), and the merged images of double labeling(c and f). (a–c) The same section of fimbria in the PBS-infused rat. (d–f) The same section of fimbria in the leupeptin-treated rat. Some cells were strongly labeled with anti-synuclein antibody only (arrows), or with anti-ubiquitin antibody only (arrowheads) (scale bar = 50 μm).

tem, leading to vicious cycle. Our results also support this hypothesis because accumulation of α-synuclein in neuronal cells was induced by leupeptin, one of well-known lysosome inhibitors, which was reported to bind with proteasome also [24]. However it is still unclear which kind of protease is predominantly involved in the accumulation of α-synuclein and formation of fibrous structures, unfortunately.

In addition to the disturbance of degradation of α-synuclein, the disturbance of axonal flow caused by leupeptin, which was demonstrated in the previous studies [28], should be taken into account as another possible mechanism in the formation of α-synuclein-positive structures.

Recently, point mutations of the α-synuclein gene at position 53 (Ala53Thr) [22] position 30 (Ala30Pro) [14] and position 46 (E46K) [33] have been detected in the families of autosomal dominant Parkinson disease patients, which may be a cause of disturbed α-synuclein metabolism. On the other hand, a marked decrease of proteasomal function by 34–42% has been reported in sporadic PD cases [18], and the degradation of mutant α-synuclein as well as of wild-type α-synuclein through the ubiquitin-proteasome system was inhibited by a selective proteasomal inhibitor, β-lactone [2]. Moreover, proteasomal activities are decreased in the *para*-hippocampal gyrus, upper-middle temporal gyri, and frontal cortex in AD cases [12]. These findings indicated that dysfunction of the ubiquitin-proteasome system may cause the accumulation of α-synuclein; however, our findings suggested that dysfunction of lysosome system or ubiquitin-independent proteasome pathway might influence the accumulation of α-synuclein [29].

Experimental α-synuclein accumulation has previously been reported in vivo [3,25]; however, previously accumulation of α-synuclein was reported in transgenic-model mouse [5,16], or rodents injected with MPTP or rotenone [3,25,30]. Both of chemical compounds were not well characterized in biochemical function on the mechanisms of cytotoxicity yet, even though oxidative stress mechanisms are thought to be mediators in either compound. This is the first report of experimentally induced in vivo accumulation of α-synuclein in non-transgenic rodent brain injected with leupeptin, a biochemically well-characterized protease inhibitor, by an infusion pump. The leupeptin infusion rat model is thought to be a useful material for studying several neuronal changes resembling the aging or degeneration of the central nervous tissue. The accumulation of α-synuclein protein in the rat brain is a finding of new interest for research on the pathogenic mechanism of neurodegeneration.

Acknowledgments

The authors are very grateful to Ms. Mina Nishimura for her technical assistance and to Ms. Bernice Miwa for English correction.

References

[1] S. Baba, S. Nakajo, P.H. Tu, T. Tomita, K. Nakaya, V.M.Y. Lee, J.Q. Trojanowski, T. Iwatsubo, Aggregation of α-synuclein in Lewy bodies of sporadic Parkinson's disease and dementia with Lewy bodies, Am. J. Pathol. 152 (4) (1998) 879–884.

[2] M.C. Bennet, J.F. Bishop, Y. Leng, P.B. Chock, T.N. Chase, M.M. Mouradian, Degradation of α-synuclein by proteasome, J. Biol. Chem. 274 (1999) 33855–33858.

[3] R. Betarbet, T.B. Sherer, G. MacKenzie, M. Garcia-Osuna, A.V. Panov, J.T. Greenamyre, Chronic systemic pesticide exposure reproduces features of Parkinson's disease, Nat. Neurosci. 3 (2000) 1301–1306.

[4] J.B. Cavanagh, C.C. Nolan, M.P. Seville, V.E.R. Anderson, P.N. Leigh, Routes of excretion of neuronal lysosomal dense bodies after ventricular infusion of leupeptin in the rat: a study using ubiquitin and PGP 9.5 immunocytochemistry, J. Neurocytol. 22 (1993) 779–791.

[5] M.B. Feany, W.W. Bender, A Drosophila model of Parkinson's disease, Nature 404 (2000) 341–343.

[6] M.C. Irizarry, W. Growdon, T. Gomez-Isla, K. Newell, J.M. George, D.F. Clayton, B.T. Hyman, Nigral and cortical Lewy bodies and dystrophic nigral neurites in Parkinson's disease and cortical Lewy body disease contain α-synuclein immunoreactivity, J. Neuropathol. Exp. Neurol. 57 (1998) 334–337.

[7] G.O. Ivy, F. Schottler, J. Wenzel, M. Baudry, G. Lynch, Inhibitors of lysosomal enzymes: accumulation of lipofuscin-like dense bodies in the brain, Science 226 (1984) 985–987.

[8] A. Iwai, E. Masliah, M. Yoshimoto, N. Ge, L. Flanagan, H.A.R. Silva, A. Kittel, T. Saitoh, The precursor protein of Non-Aβ component of Alzheimer's disease amyloid is a presynaptic protein of the central nervous system, Neuron 14 (1995) 467–475.

[9] R. Jakes, M.G. Spillantini, M. Goedert, Identification of two distinct synucleins from human brain, FEBS Lett. 345 (1993) 27–32.

[10] N.R. Jana, E.A. Zemskov, G.h. Wang, N. Nukina, Altered proteasomal function due to the expression of polyglutamine-expanded truncated N-terminal huntingtin induces apoptosis by caspase activation through mitochondrial cytochrome c release, Hum. Mol. Genet. 10 (2001) 1049–1059.

[11] E. Junn, S.S. Lee, U.T. Suhr, M.M. Mouradian, Parkin accumulation in aggresomes due to proteasome impairment, J. Biol. Chem. 277 (2002) 47870–47877.

[12] J.N. Keller, K.B. Hanni, W.R. Markesbery, Impaired proteasome function in Alzheimer's disease, J. Neurochem. 75 (2000) 436–439.

[13] K. Kosaka, Diffuse Lewy body disease in Japan, J. Neurol. 237 (1990) 197–204.

[14] R. Krüger, W. Kuhn, T. Müller, D. Woitalla, M. Graeber, S. Kösel, H. Przuntek, J.T. Epplen, L. Schöls, O. Riess, Ala30Pro mutation in the gene encoding α-synuclein in Parkinson's disease, Nat. Genet. 18 (1998) 106–108.

[15] H.J. Lee, S.J. Lee, Characterization of cytoplasmic alpha-synuclein aggregates. Fibril formation is tightly linked to the inclusion-forming process in cells, J. Biol. Chem. 277 (2002) 48976–48983.

[16] E. Masliah, E. Rockenstein, I. Veinbergs, M. Mallory, M. Hashimoto, A. Takeda, Y. Sagara, A. Sisk, L. Mucke, Dopaminergic loss and inclusion body formation in alpha-synuclein mice: implications for neurodegenerative disorders, Science 287 (2000) 1265–1269.

[17] E. Masliah, A. Iwai, M. Mallory, K. Ueda, T. Saitoh, Altered presynaptic protein NACP is associated with plaque formation and neurodegeneration in Alzheimer's disease, Am. J. Pathol. 148 (1996) 201–210.

[18] K.S.P. McNaught, P. Jenner, Proteasomal function is impaired in substantia nigra in Parkinson's disease, Neurosci. Lett. 297 (2001) 191–194.

[19] A. Musial, T. Eissa, Inducible nitric-oxide synthase is regulated by the proteasome degradation pathway, J. Biol. Chem. 276 (2001) 24268–24273.

[20] R.J. Perrin, J.E. Payton, D.H. Barnett, C.L. Wraight, W.S. Woods, L. Ye, J.M. George, Epitope mapping and specificity of the anti-α-synuclein monoclonal antibody Syn-1 in mouse brain and cultured cell lines, Neurosci. Lett. 349 (2003) 133–135.

[21] K. Petersen, O.F. Olesen, J.D. Mikkelsen, Developmental expression of alpha-synuclein in rat hippocampus and cerebral cortex, Neuroscience 91 (1999) 651–659.

[22] M.H. Polymeropoulos, C. Lavedan, E. Leroy, S.E. Ide, A. Dehejia, A. Dutra, B. Pike, H. Root, J. Rubenstein, R. Boyer, E.S. Stenroos, S. Chandrasekharappa, A. Athanassiadou, T. Papapetropoulos, W.G. Johnson, A.M. Lazzarini, R.C. Duvoisin, G. Di Iorio, L.I. Golbe, R.L. Nussbaum, Mutations in the α-synuclein identified families with Parkinson's disease, Science 276 (1997) 2045–2048.

[23] H.J. Rideout, K.E. Larsen, D. Sulzer, L. Stefanis, Proteasomal inhibition leads to formation of ubiquitin/α-synuclein-immunoreactive inclusions in PC12 cells, J. Neurochem. 78 (2001) 899–908.

[24] P.J. Savory, A.J. Rivett, Leupeptin-binding site(s) in the mammalian multicatalytic proteinase, Biochem. J. 289 (1993) 45–48.

[25] T.B. Sherer, J.H. Kim, R. Betarbet, J.T. Greenamyre, Subcutaneous rotenone exposure causes highly selective dopaminergic degeneration and α-synuclein aggregation, Exp. Neurol. 179 (2003) 9–16.

[26] M.G. Spillantini, M.L. Schmidt, V.M.Y. Lee, J.Q. Trojanowski, R. Jakes, M. Goedert, α-Synuclein in Lewy bodies, Nature 388 (1997) 838–840.

[27] S. Takauchi, K. Miyoshi, Degeneration of neuronal processes in rats induced by a protease inhibitor, leupeptin, Acta Neuropathol. 78 (1989) 380–387.

[28] S. Takauchi, K. Miyoshi, Cytoskeletal changes in rat cortical neurons induced by long-term intraventricular infusion of leupeptin, Acta Neuropathol. 89 (1995) 8–16.

[29] G.K. Tofaris, R. Layfield, M.G. Spillantini, Alpha-synuclein metabolism and aggregation is linked to ubiquitin-independent degradation by the proteasome, FEBS Lett. 509 (2001) 22–26.

[30] M. Vila, S. Vukosavic, V. Jachson-Lewis, M. Neystat, M. Jakowec, S. Przedborski, α-Synuclein up-regulation in substantia nigra dopaminergic neurons following administration of the Parkinsonian toxin MPTP, J. Neurochem. 74 (2000) 721–729.

[31] K. Wakabayashi, M. Yoshimoto, S. Tsuji, H. Takahashi, α-Synuclein immunoreactivity in glial cytoplasmic inclusions in multiple system atrophy, Neurosci. Lett. 249 (1998) 180–182.

[32] O. Yokota, S. Terada, H. Ishizu, K. Tsuchiya, Y. Kitamura, K. Ikeda, K. Ueda, S. Kuroda, NACP/α-synuclein immunoreactivity in diffuse neurofibrillary tangles with calcification (DNTC), Acta Neuropathol. 104 (2002) 333–341.

[33] J.J. Zarranz, J. Alegre, J.C. Gomez-Esteban, E. Lezcano, R. Ros, I. Ampuero, L. Vidal, J. Hoenicka, O. Rodriguez, B. Atares, V. Llorens, E.G. Torrosa, T. Ser, D.G. Munoz, J.G. Yebenes, The new mutation, E46K, of a-synuclein causes Parkinson and Lewy body dementia, Ann. Neurol. 55 (2004) 164–173.

Amyloid-β down-regulates XIAP expression in human SH-SY5Y neuroblastoma cells

Hidenaga Yamamori, Toshihisa Tanaka[CA], Takashi Kudo and Masatoshi Takeda

Division of Psychiatry and Behavioral Proteomics, Department of Post-Genomics and Diseases, Course of Advanced Medicine, Osaka University, Graduate School of Medicine. D-3, 2-2 Yamadaoka, Suita, Osaka 565-0871, Japan

[CA]Corresponding Author: tanaka@ psy.med.osaka-u.ac.jp

Received 26 December 2003; accepted 29 January 2004

DOI: 10.1097/01.wnr.0000121231.63082.8a

Recent observations suggest that amyloid-β (Aβ), a major constituent of senile plaques, induces apoptosis in cultured neuronal cells. However, the concentration of Aβ that leads to neuronal cell death is much higher (10–25 μM) than that in the cerebrospinal fluid of normal controls or AD patients (nM order). As reported here, we found that subtoxic concentrations (100–500 nM) of Aβ(1-42) can down-regulate the expression of the X-linked inhibitor of apoptosis (XIAP) in human SH-SY5Y neuroblastoma cells, and that vulnerability to oxidative stress caused by Aβ(1-42) is attenuated by over-expression of XIAP. These results suggest that down-regulation of XIAP expression in response to subtoxic, more physiological concentrations (100–500 nM) of Aβ(1-42) increases vulnerability to oxidative stress. *NeuroReport* 15:851–854 © 2004 Lippincott Williams & Wilkins.

Key words: Alzheimer's disease (AD); Amyloid β (Aβ); Apoptosis; Oxidative stress; X-linked inhibitor of apoptosis (XIAP)

INTRODUCTION

Alzheimer's disease (AD) is a progressive neurodegenerative disorder, characterized by extracellular senile plaques that are composed of the deposition of amyloid-β (Aβ), the formation of neurofibrillary tangles, with abnormally phosphorylated tau as their major component, and a reduction in neuronal cells. Aβ is a 39–43 amino acid peptide derived from processing of the amyloid precursor protein (APP). The importance of Aβ in the pathogenesis of AD has been indicated by several findings. Most important, mutations in presenilin-1, -2 and APP, which are involved in familial forms of AD, lead to an increase in the amyloidogenic form of Aβ [1]. Although it is still controversial whether this increase in Aβ formation is sufficient to cause nerve cell degeneration in AD, the neurotoxic effects of Aβ have been demonstrated both *in vitro* and *in vivo* [2–5]. Recent studies have also shown that in cultures of neurons exposed to Aβ, dying cells display the characteristics of apoptosis [6]. It has been suggested that Aβ-induced apoptosis involves oxidative stress and perturbation of intracellular calcium homeostasis [3,7]. However, the Aβ concentration that leads to apoptosis is much higher (10–25 μM) than the physiological concentration (nM order).

Apoptosis is regulated by several gene products, including the members of the caspase family, Apaf-1 and related proteins, the Bcl-2 family, and the inhibitor of apoptosis (IAP) family [8–11]. Members of the IAP family are intrinsic cellular suppressors of apoptosis and are represented by highly conserved members found in a wide range of locations, from insect viruses to mammals. The most potent human IAP is the X-linked inhibitor of apoptosis (XIAP), whose mechanism of action involves direct inhibition of caspase 3, 7 and 9, which are key proteases of the apoptotic cascade. Furthermore, XIAP is ubiquitously expressed, whereas expression of HIAP1 or HIAP2 is lowest in the CNS [11]. Given the potency of XIAP as inhibitor of apoptosis and previous findings that subtoxic, high physiological concentrations of Aβ increases vulnerability to oxidative stress, at least in part through an increase in the expression ratio of Bax/Bcl-2 [13], we decided to examine the effects of subtoxic concentrations of Aβ on the expression of XIAP.

MATERIALS AND METHODS

Preparation of gene construct: The XIAP gene, a gift from Dr J.D. Ashwell (National Institute of Health, Bethesda, USA), was cut with *Bam*HI and *Not*I restriction enzymes and inserted with a linker into the pcDNA3.1(+) (Invitrogen, Carlsbad, CA, USA) vector cut with *Nhe*I and *Not*I.

Cell line, culture conditions, and transfections: SH-SY5Y human neuroblastoma cells were kindly donated by Dr J.L. Biedler (Sloan Kettering Institute, New York, NY, USA) and were cultured in DMEM/F12 containing 5% fetal calf serum (FCS). Cultures were transfected with the XIAP gene or a mock vector gene employing optimum-minimum essential medium with Lipofectamine2000 (Gibco, Rockville, MD, USA). Stably transfected cells were selected in 600 μg/ml G418 (Invitrogen, Carlsbad, CA, USA) for 3 weeks. Pools of ~100 colonies were used to avoid bias of single cell colonies.

Treatment of cell cultures with Aβ: Fibrillar Aβ1-42 (Sigma-Aldrich, Tokyo, Japan) and control reverse peptide Aβ42-1 (BACHEM, King of Prussia, PA, USA) were prepared by incubation at 200 μM in sterile water at 37°C for 3 days.

Cells were plated for 3 days before treatment with Aβ. Confluent cultures (about 60% confluence) were used and were placed in fresh media 2 h before treatment. Aβ peptides were added to the cultures and incubated for 12, 24 and 48 h.

Oxidative stress on cell cultures pre-exposed to Aβ: Cells were treated for 48 h with fibrillar Aβ1-42 (500 nM) as described above. H_2O_2 (0.5 μM) or 5 nM 4-hydroxynonenal (HNE) was then added to the cultures and incubated for 3 h.

Cell viability assay: Surviving and dead cells were visualized and counted in three fields (600–700 cells) per well in a blinded manner with the aid of the Live/Dead Eukolight Viability/Cytotoxicity Kit (Molecular Probes, Eugene, OR, USA). Data show dead cells as a percentage of total cells.

Assessment of caspase activity: Analysis of caspase activity was performed with the Caspase Colorimetric Protease Assay Kit according to the manufacturer's instructions (MBL, Nagoya, Japan). After exposure to Aβ and oxidative stress, the culture medium was aspirated, and the cells washed with phosphate buffered saline, lysed in lysis buffer, and centrifuged at 10 000 × *g* for 10 min. Aliquots of 100 μg supernatant were added to the reaction buffer and incubated at 37°C for 2 h. The reaction buffer was supplemented with 200 μM DEVD-pNA, a colorimetric substrate for caspase-3 and -7. Production of pNA was monitored with a microplate reader at an absorbance of 405 nm. Colorimetric blanks containing no cellular extracts were subtracted from the values obtained.

Antibodies: Anti-XIAP polyclonal antibody was purchased from R&D Systems (Minneapolis, MN, USA) and Anti-Actin polyclonal antibody from Sigma-Aldrich (Tokyo, Japan).

Western blots: Cells were lysed in 100 mM PIPES pH 6.8, 2 mM $MgCl_2$, 0.1 mM EDTA, 1 mM PMSF, 5 μg/ml aprotinine, 5 μg/ml leupeptine, 25 mM NaF, 1 mM Na_3VO_4, 0.1% Triton-X100 on ice, and centrifuged at 200 000 × *g* for 30 min. The supernatants were used for Western blot analysis. Aliquots of 50 μg supernatant were separated by SDS-PAGE and transferred to nitrocellulose membranes. Peroxidase-labeled anti-rabbit IgG was used as the secondary antibody, and membranes were developed by means of ECL (Amersham Biosciences, Buckinghamshire, UK).

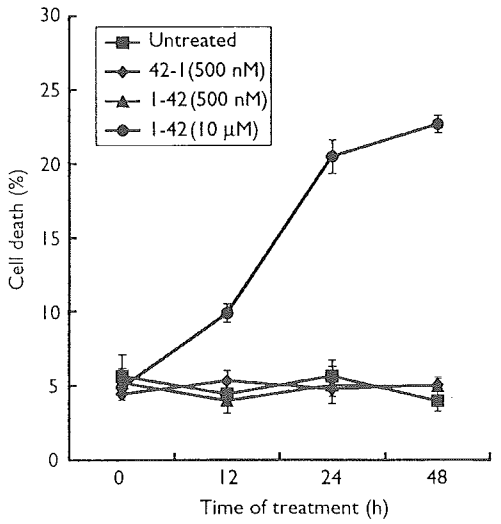

Fig. 1. Cell death in SH-SY5Y cells treated with Aβ. Fibrillar Aβ1-42 (500 nM) did not cause high levels of cell death in SH-SY5Y cells. SH-SY5Y cells were exposed to fibrillar Aβ1-42 (500 nM and 10 μM), and Aβ42-1 (500 nM) for 12 h, 24 h, and 48 h. Surviving and dead cells were visualized and counted with the Live/Dead Eukolight Viability/Cytotoxicity Kit. Data show dead cells as a percentage of total cells (n=3, mean ± s.e.m.).

RESULTS

Cell death in SH-SY5Y cells treated with Aβ: SH-SY5Y cell death after exposure to Aβ was quantified by calsein

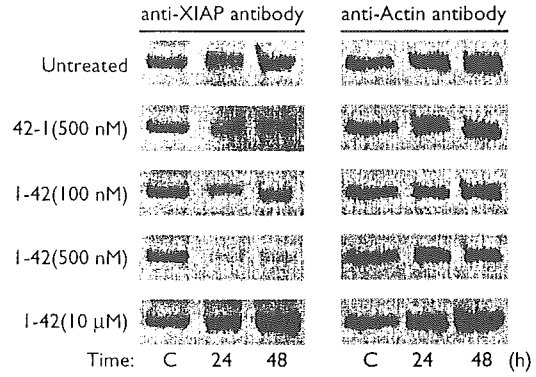

Fig. 2. Western blot analysis showing expression of XIAP and Actin after treatment with Aβ. Concentration-dependent down-regulation of XIAP expression by fibrillar Aβ1-42 at subtoxic concentrations. SH-SY5Y cells were treated with fibrillar Aβ1-42 (100 nM, 500 nM and 10 μM) and Aβ42-1 (500 nM) for the indicated number of hours.

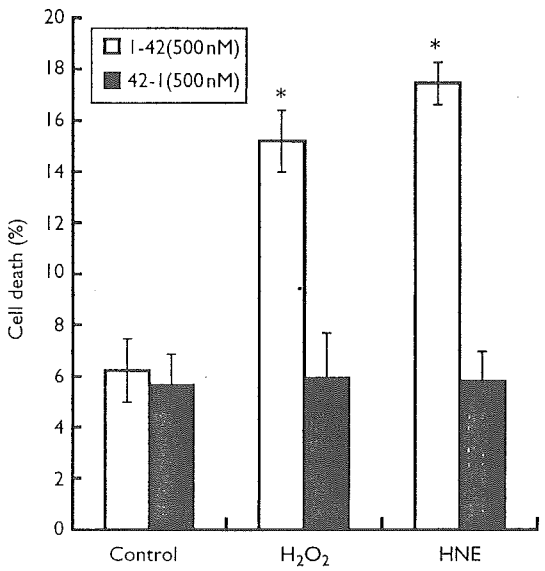

Fig. 3. Susceptibility to oxidative stress in SH-SY5Y cells pretreated with fibrillar Aβ1-42 but not in those pretreated with Aβ42-1. EthD-1 staining indicates increased cell death in cells pretreated with fibrillar Aβ1-42 (500 nM) for 48 h and then submitted to low oxidative stress levels, by exposure to 0.5 μM H_2O_2 or 5 nM HNE. In contrast, the cells treated with the control peptide Aβ42-1 (500 nM) did not show an increase in sensitivity to low levels of oxidative stress. Data show dead cells as a percentage of total cells (n=3, mean ± s.e.m.). *$p < 0.05$: significantly different from respective controls (two sample t-test).

acetoxymethylester/EthD-1 double staining. Uptake of EthD-1 indicates membrane leakage, a terminal stage of neuronal degeneration, which also occurs after neuronal apoptosis. There was no significant difference between fibrillar Aβ1-42 (500 nM), Aβ42-1 (500 nM), and untreated cells. Fibrillar Aβ1-42 (500 nM) did not cause high levels of cell death in SH-SY5Y cells, although in cells treated with 10 μM fibrillar Aβ1-42, an increase in cell death with time was observed (Fig. 1).

Aβ down-regulates XIAP expression: To determine whether XIAP expression is involved in the Aβ-induced neurotoxic mechanism, the expression level of XIAP protein in SH-SY5Y cells exposed to Aβ was investigated by western blotting. Treatment with fibrillar Aβ1-42 at subtoxic concentrations (100–500 nM) reduced XIAP protein levels in a concentration-dependent manner compared to cells treated with Aβ42-1 control and untreated cells. Fibrillar Aβ1-42 at a toxic dose (10 μM) did not down-regulate but could have induced XIAP expression (Fig. 2).

XIAP attenuates vulnerability to oxidative stress: To determine whether cells exposed to Aβ were more vulnerable to an age-dependent secondary insult such as oxidative stress, we first treated the SH-SY5Y cells with subtoxic (500 nM) Aβ1-42 for 48 h and then used 0.5 μM. H_2O_2 or 5 nM HNE to expose them to low oxidative stress levels. The Aβ-treated cells proved to be more vulnerable to oxidative stress than untreated cells (Fig. 3, Fig. 4b).

To determine whether XIAP expression is involved in the mechanism of this Aβ-induced increase in vulnerability to

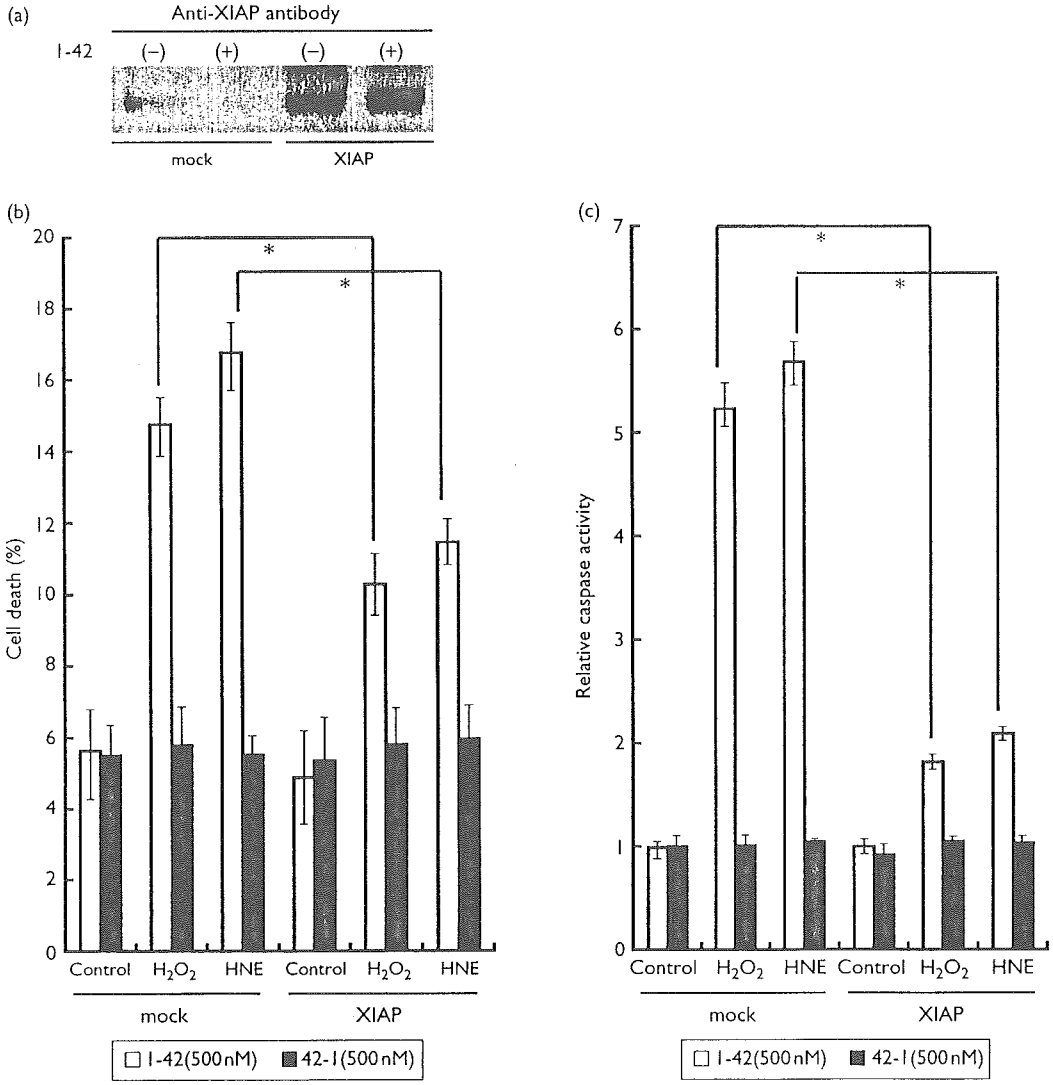

Fig. 4. XIAP attenuates vulnerability to oxidative stress. **(a)** The levels of XIAP expression in transfected cell lines were determined by Western blotting. In cells showing over-expression of XIAP, no change was observed after treatment with fibrillar Aβ1-42 (500 nM) for 48 h. **(b)** Susceptibility to oxidative stress in SH-SY5Y cells pretreated with fibrillar Aβ1-42 was attenuated by over-expression of XIAP. SH-SY5Y cells were stably transfected with the XIAP gene or a mock vector gene and exposed to 0.5 μM H_2O_2 or 5 nM HNE after treatment with fibrillar Aβ1-42 (500 nM) or control peptide Aβ42-1 (500 nM) for 48 h. Surviving and dead cells were visualized and counted with the Live/Dead Eukolight Viability/Cytotoxicity Kit. Data show dead cells as a percentage of total cells (n=3, mean ± s.e.m.). *$p < 0.05$: significantly different from mock (two sample t-test). **(c)** Activation of caspase activity induced by oxidative stress after treatment with Aβ was inhibited by over-expression of XIAP. Caspase activity was measured by observing the cleavage of DEVD-pNA, the colorimetric substrate for caspase-3 and -7. Data show caspase activity in cells relative to that in Aβ42-1 treated cells transfected with the mock vector gene (n=3, mean ± s.e.m.). *$p < 0.05$: significantly different from mock (two sample t-test).

oxidative stress, we studied the effect of overexpression of XIAP on oxidative stress resistance. SH-SY5Y cells were stably transfected with a mock vector gene or the XIAP gene (Fig. 4a) and exposed to 0.5 μM H_2O_2 or 5 nM HNE after treatment with Aβ1-42 for 48 h. Vulnerability to oxidative stress caused by Aβ at a subtoxic concentration (500 nM) was attenuated by over-expression of XIAP (Fig. 4b). To further investigate the relationship between the attenuation of vulnerability and inhibition of caspase activity by XIAP, caspase activity was measured by observing the cleavage of DEVD-pNA, the colorimetric substrate for caspase-3 and -7. Activation of caspase activity induced by oxidative stress after treatment with Aβ was found to be inhibited by over-expression of XIAP (Fig. 4c). This led to the hypothesis that over-expression of XIAP attenuates vulnerability to oxidative stress, in part through inhibition of caspases.

DISCUSSION

Aβ is a major constituent of senile plaques, which are a hallmark of AD, and the production of Aβ might be a primary cause of neuronal cell death that leads to cognitive dysfunction in AD [1]. Recent observations suggest that Aβ induces apoptosis in cultured neuronal cells [6], and that the concentration of Aβ that leads to neuronal cell death is much higher than that observed in the cerebrospinal fluid of normal controls or AD patients [3,4,6,7]. Bax is a pro-apoptotic and Bcl-2 an anti-apoptotic factor involved in the process of apoptosis [9]. It has been reported that subtoxic concentrations of Aβ increase vulnerability to oxidative stress, at least in part through an increase in the expression ratio of Bax/Bcl-2 [13].

In this study we examined the possibility that Aβ at a subtoxic, more physiological concentration increases vulnerability to age-dependent secondary insults such as oxidative stress through changing the expression of XIAP. Aβ at subtoxic concentrations was found to down-regulate XIAP expression (Fig. 1, Fig. 2). Furthermore, over-expression of XIAP attenuated vulnerability to oxidative stress caused by subtoxic concentrations of Aβ (Fig. 3, Fig. 4). An increase in the XIAP protein level was observed in cells treated with Aβ at a toxic dose. Expression of the XIAP protein is translationally regulated via internal ribosome entry site (IRES) elements located in the 5′ untranslated region (5′UTR) [14] and IRES-regulated proteins are synthesized under a variety of stress conditions, including hypoxia, serum deprivation, amino acid deficiency, and apoptosis [12,15,16]. The increase in the XIAP protein level observed in cells treated with toxic Aβ is therefore thought to be caused by Aβ-induced apoptosis. It remains unclear how Aβ down-regulates XIAP expression. Recently, it was reported that degradation of XIAP is mediated by proteasome or calpain [17,18]. It is possible that in cells treated with Aβ, XIAP has readily been degraded by activation of proteasome or calpain. It is also possible that the IRES-regulated synthesis of XIAP is interfered with in cells treated with Aβ. Further study is needed to determine how Aβ down-regulates XIAP expression.

CONCLUSION

Our findings suggest that down-regulation of XIAP expression in response to Aβ at subtoxic, more physiological concentrations increases vulnerability to oxidative stress. When combined with the observation of an increase in the expression ratio of Bax/Bcl-2, these findings may offer an explanation for the neurodegenerative mechanisms of AD caused by low concentrations of Aβ.

REFERENCES

1. Selkoe DJ. Translating cell biology into therapeutic advances in Alzheimer's disease. *Nature* **399**, A23–A31 (1999).
2. Geula C, Wu CK, Saroff D, Lorenzo A, Yuan M and Yankner BA. Aging renders the brain vulnerable to amyloid β-protein neurotoxicity. *Nature Med* **4**, 827–831 (1998).
3. Mattoson MP, Cheng B, Davis D, Bryant K, Lieberburg I and Rydel RE. β-Amyloid peptides destabilize calcium homeostasis and render human cortical neurons vulnerable to excitotoxicity. *J Neurosci* **12**, 376–389 (1992).
4. Hartley DM, Walsh DM, Ye CP, Diehl T, Vasquez S, Vassilev PM *et al.* Protofibrillar intermediates of amyloid β-protein induce acute electrophysiological changes and progressive neurotoxicity in cortical neurons. *J Neurosci* **19**, 8876–8884 (1999).
5. Walsh DM, Klyubin I, Fadeeva JV, Cullen WK, Anwyl R, Wolfe MS *et al.* Naturally secreted oligomers of amyloid β protein potently inhibit hippocampal long-term potentiation *in vivo*. *Nature* **416**, 535–539 (2002).
6. Estus S, Tucker HM, van Rooyen C, Wright S, Brigham EF, Wogulis M *et al.* Aggregated amyloid-β protein induces cortical neuronal apoptosis and concomitant apoptotic pattern of gene induction. *J Neurosci* **17**, 7736–7745 (1997).
7. Behl C, Davis JB, Lesley R and Schubert D. Hydrogen peroxide mediates amyloid β protein toxicity. *Cell* **77**, 817–827 (1994).
8. Nicholson DW and Thornberry NA. Caspase: killer proteases. *Trends Biochem Sci* **22**, 299–306 (1997).
9. Reed JC. Bcl-2 family proteins. *Oncogene* **17**, 3225–3236 (1998).
10. Zou H, Henzel WJ, Liu X, Lutschg A and Wang X. Apaf-1, a human protein homologous to *C. elegans* CED-4, participates in cytochrome c-dependent activation of caspase-3. *Cell* **90**, 405–413 (1997).
11. Deveraux QL and Reed JC. IAP family proteins-suppressors of apoptosis. *Genes Dev* **13**, 239–252 (1999).
12. Katz LM, Lotocki G, Wang Y, Kraydieh S, Dietrich WD and Keane RW. Regulation of caspases and XIAP in the brain after asphyxial cardiac arrest in rats. *Neuroreport* **12**, 3751–3754 (2001).
13. Paradis E, Douillard H, Koutroumanis M, Goodyer C and LeBlanc A. Amyloid β peptide of Alzheimer's disease down-regulates Bcl-2 and up-regulates bax expression in human neurons. *J Neurosci* **16**, 7533–7539 (1996).
14. Holcik M, Lefebvre C, Yeh C, Chow T and Korneluk RG. A new internal-ribosome-entry-site motif potentiates XIAP-mediated cytoprotection. *Nature Cell Biol* **1**, 190–192 (1999).
15. Holcik M, Sonenberg N and Korneluk RG. Internal ribosome initiation of translation and the control of cell death. *Trends Genet* **16**, 469–473 (2000).
16. Fernandez J, Yaman I, Mishra R, Merrick WC, Snider MD, Lamers WH *et al.* Internal ribosome entry site-mediated translation of a mammalian mRNA is regulated by amino acid availability. *J Biol Chem* **276**, 12285–12291 (2001).
17. Yang Y, Fang S, Jensen JP, Weissman AW and Ashwell JD. Ubiquitin protein ligase activity of IAPs and their degradation in proteasomes in response to apoptotic stimuli. *Science* **288**, 874–877 (2000).
18. Kobayashi S, Yamashita K, Takeoka T, Ohtsuki T, Suzuki Y, Takahashi R *et al.* Calpain-mediated X-linked inhibitor of apoptosis degradation in neutrophil apoptosis and its impairment in chronic neutrophil leukemia. *J Biol Chem* **277**, 33968–33977 (2002).

Acknowledgements: We thank Dr J.D. Ashwell for providing vectors. This work was supported by grants 14570922 and 15390351 from the Ministry of Education, Culture, Sports, Science and Technology, Japan.

Takeda M, Tanaka T, Cacabelos R (eds): Molecular Neurobiology of Alzheimer Disease and Related Disorders. Basel, Karger, 2004, pp 225–235

Activated Protein Kinases and Phosphorylated Tau Protein in Alzheimer Disease

Toshihisa Tanaka[a], *Hidenaga Yamamori*[a], *Kenji Wada-Isoe*[b], *Ichiro Tsujio*[a], *Masatoshi Takeda*[a]

[a] Psychiatry and Behavioral Science, Osaka University, Graduate School of Medicine, Yamadaoka, Suita, Osaka,
[b] Division of Neurology, Faculty of Medicine, Tottori University, Nishimachi, Yonago, Tottori, Japan

Neurofibrillary tangles of paired helical filaments (PHF) are neuropathological hallmarks of Alzheimer disease (AD), and abnormally hyperphosphorylated tau protein is the major protein subunit of PHF [1–4]. Several kinases and phosphatases are thought to be involved in the process [5–11]. However, the mechanisms of phosphorylation of tau protein and neurodegeneration in AD are still unclear.

In this review, phosphorylation of tau protein and the recently found activated protein kinases in AD are overviewed and their involvement in the formation of phosphorylated tau protein and in the neurodegenerative process of AD are discussed.

Phosphorylation of Tau Protein

Tau protein has six isoforms which derive from a single gene by an alternative splicing mechanism, and the longest isoform is composed of 441 amino acids [12] (fig. 1). An alternative splicing mechanism produces tau with two, one and no N-terminal insertion(s); it also produces tau with and without an insertion in microtubule binding domains. Isoforms with an insertion in microtubule binding domains are called 4-repeats tau, and the others are called

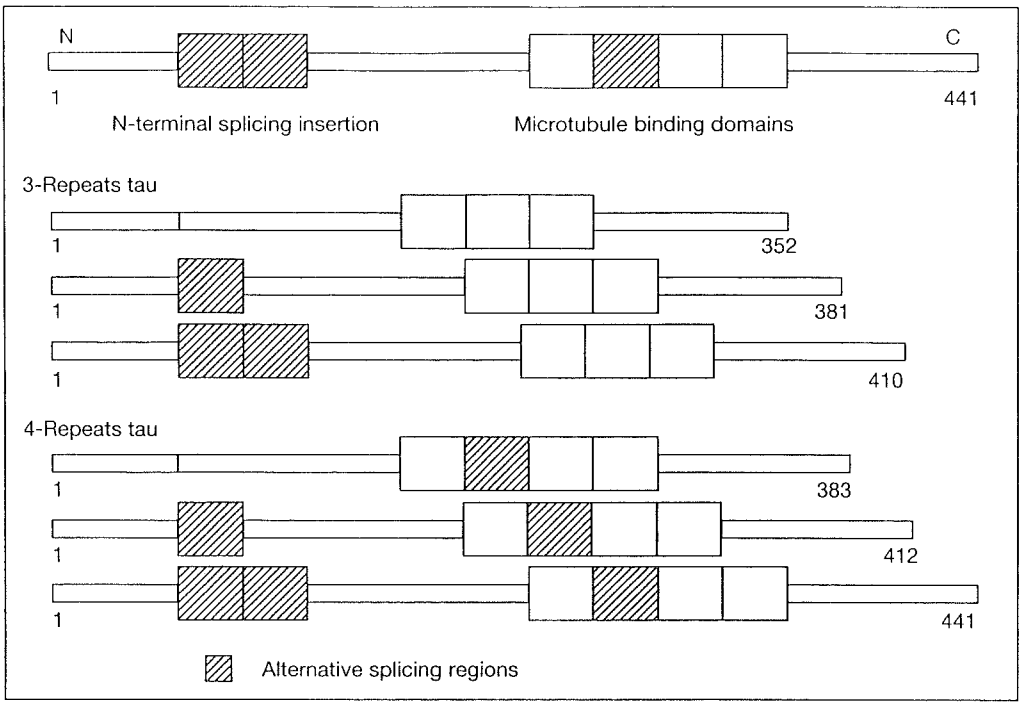

Fig. 1. Structure of tau protein. Tau protein consists of six isoforms which derive from a single gene by an alternative splicing mechanism; the isoforms are composed of 352, 381, 383, 410, 412, and 441 amino acids, respectively. An alternative splicing mechanism produces tau with two, one and no N-terminal insertion(s); it also produces tau with and without an insertion in microtubule binding domains. Isoforms with an insertion in microtubule binding domains are called 4-repeat tau, and others are called 3-repeat tau. Hatched squares indicate alternative splicing regions.

3-repeat tau. The expression of these isoforms is developmentally regulated; fetal tau consists of only 3-repeat tau and adult tau consists of all six isoforms [13]. Tau protein is one of the microtubule-associated proteins and has an ability to promote microtubule assembly. This activity is regulated by phosphorylation, which impairs the ratio of microtubule assembly [14].

Tau protein in normal brain contains 1–2 mol of phosphate(s) per 1 mol of tau protein; however in AD brains, tau protein contains 5–9 mol of phosphates [15]. This abnormal phosphorylated tau protein is present in the affected neurons as amorphous aggregates [16]. Phosphorylation of many Ser/Thr sites on tau protein has already been reported (fig. 2). Among 27 phosphorylated Ser/Thr sites on tau protein in AD, 11 sites are proline-directed (-Ser/Thr-Pro-) sites [17]. Therefore proline-directed protein kinases have been thought to be important in abnormal phosphorylation of tau protein in AD.

Among proline-directed kinases, glycogen synthase kinase-3 (GSK-3) is one of the important kinases in the phosphorylation of tau protein. GSK-3

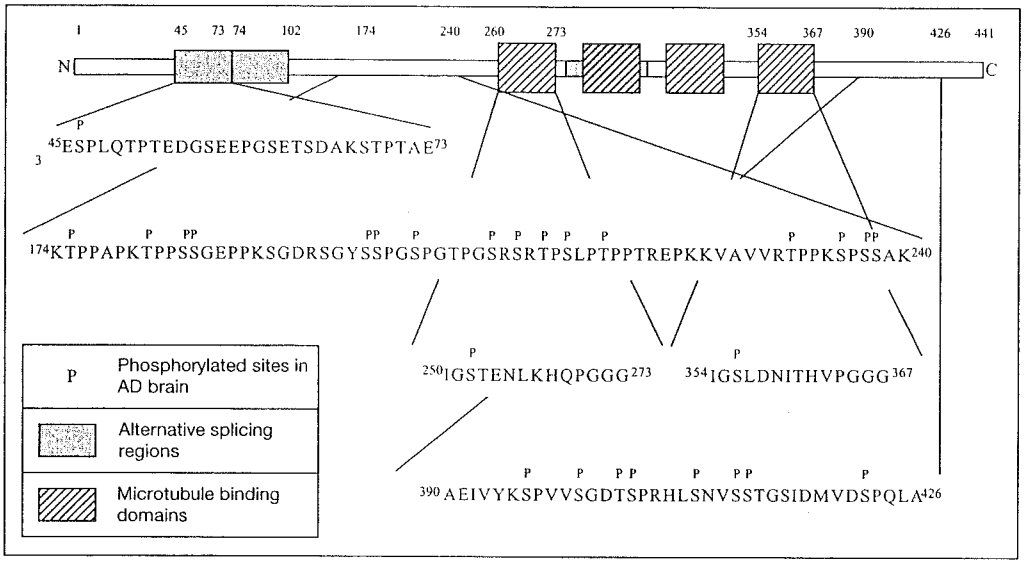

Fig. 2. Phosphorylated sites in an AD brain. The structure of tau is the longest isoform, and P associated with Ser/Thr indicates a phosphorylated site. Gray and hatched boxes indicate alternative splicing regions and microtubule binding domains, respectively.

strongly phosphorylates tau protein in vitro, and is localized in axons [18, 19]. And in fact, previously reported tau protein kinase-I was identified as GSK-3β [20, 21].

Regulation of Activity of GSK-3

GSK-3 is a calcium- and cyclic nucleotide-independent kinase that phosphorylates glycogen synthase, a regulatory enzyme of glycogen. The molecular weights of the α- and β-isoforms are 51 and 46 kD, respectively, and both are known to be able to phosphorylate tau protein [20, 21]. Protein phosphatase-I, G-subunit, the RII subunit of cyclic AMP-dependent protein kinase, phosphatase inhibitor-2, myelin basic protein and neurofilaments are known as substrates for GSK-3 [22–25]. The phosphorylation of GSK-3 regulates its activity and it has been reported that phosphorylation at Tyr 216 and nonphosphorylation at Ser9 are necessary for the activation of GSK-3β [26–28]. The consensus sequence of GSK-3 for phosphorylation is not only proline-directed Ser/Thr, but also Ser-X-X-X-Ser(p) [Ser(p) is prephosphorylated Ser] [29]. Glycogen synthase, β-catenine and tau protein contain Ser/Thr-X-X-X-Ser/Thr sequences and this implies that these proteins have potential sites for phosphorylation by GSK-3 after prime phosphorylation by other kinases [29–31].

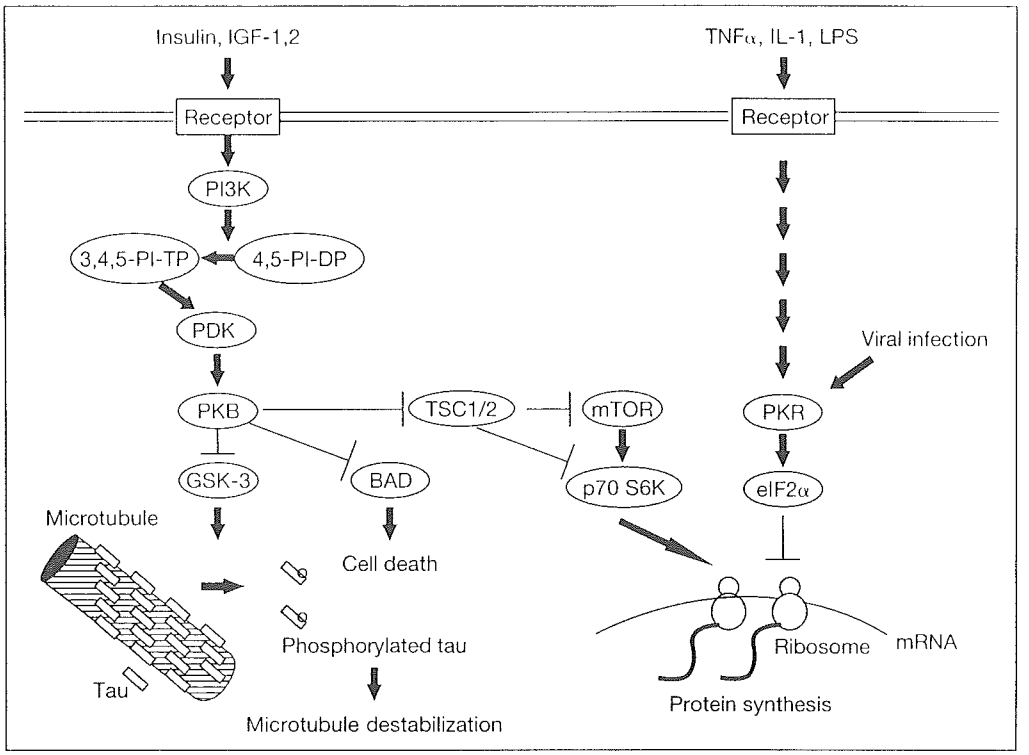

Fig. 3. Intracellular signal transduction on the activated kinases in an AD brain. The PI3K pathway is shown on the left. Binding of insulin, IGF-1 or 2, to the receptor leads to autophosphorylation of the receptor, and PI3K is activated by its binding to the receptor. Activated PI3K converts 4,5-PI-DP to 3,4,5-PI-TP. PDK is activated by its binding with 3,4,5-PI-TP and phosphorylates PKB. Activated PKB (by its phosphorylation) phosphorylates GSK-3 and inhibits the kinase activity of GSK-3. GSK-3 strongly phosphorylates tau protein and phosphorylated tau protein is detached from microtubules, leading to destabilization of microtubules. Then active PKB inhibits tau phosphorylation and microtubule destabilization. In addition, active PKB phosphorylates BAD, a proapoptotic protein, and phosphorylated BAD leads to inhibition of apoptosis. Further active PKB phosphorylates components of TSC, TSC1 and TSC2, and phosphorylation of TSC1/2 inhibits its inhibitory potency to activation of p70 S6K by mammalian target of rapamycin (mTOR). Therefore active PKB accelerates the activation of p70 S6K by mTOR, leading to activation of protein synthesis. On the right, regulation of eIF2α and PKR, and dsRNA-activated protein kinase are shown. TNFα, IL-1 and lipopolysaccharide (LPS) bind their receptors, and induce the expression of PKR; viral infection also activates PKR. Activated PKR phosphorylates eIF2α, and phosphorylated eIF2α inhibits the translational machinery.

The regulation of the signal transduction cascade has been studied, and regulatory mechanisms of GSK-3 have already been identified (fig. 3). The predominant regulatory system of the activity of GSK-3 is the phosphatidylinositol-3 kinase (PI3K) pathway, which is stimulated by insulin, IGF-1 or -2 [32]. The binding of insulin, IGF-1 or -2, to the receptor leads to autophosphorylation of

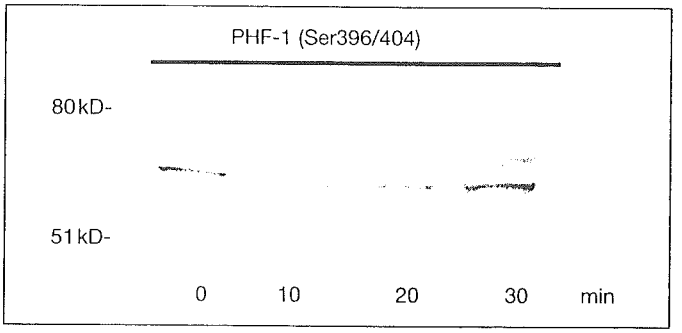

Fig. 4. Phosphorylation levels of tau protein in SH-SY5Y neuroblastoma cells treated with insulin. SH-SY5Y human neuroblastoma cells were treated with 250 μg/ml of insulin and the levels of phosphorylation of tau protein were investigated employing PHF-1 antibody that reacted with tau phosphorylated at Ser396/404. The intensities of bands decreased within 10–20 min, suggesting that dephosphorylation of tau protein was induced. The effect of insulin disappeared after 30 min.

the receptor, and PI3K is activated by its binding to the receptor. Activated PI3K converts 4,5-phosphatidylinositol diphosphate (4,5-PI-DP) to 3,4,5-phosphatidylinositol triphosphate (3,4,5-PI-TP). Phosphatidylinositol-dependent kinase (PDK) is activated by its binding with 3,4,5-PI-TP, and phosphorylates protein kinase B (PKB). Activated PKB (by its phosphorylation) phosphorylates GSK-3, and inhibits the kinase activity of GSK-3 [32]. In addition, active PKB phosphorylates BAD, a pro-apoptotic protein, and phosphorylated BAD is sequestrated from mitochondria, leading to inhibition of apoptosis [33, 34]. Therefore activation of PKB plays an important role in inhibition of apoptosis. Taken together insulin, IGF-1 or -2, is able to reduce the phosphorylation of tau protein through inhibition of GSK-3 and to lead to cell survival.

The level of phosphorylation of tau protein was regulated by this pathway. SH-SY5Y human neuroblastoma cells were treated with 250 μg/ml of insulin and the levels of phosphorylation of tau protein was investigated employing PHF-1 antibody that reacted with tau phosphorylated at Ser396/404 (fig. 4). Insulin is thought to activate the PI3K pathway that reduces the activity of GSK-3. Dephosphorylation of tau protein was induced with 10–20 min, and after 30 min the effect of insulin disappeared.

To observe the role of PI3K in the regulation of tau phosphorylation, wortmannin, an inhibitor of PI3K, was employed in our previous investigation [35]. And increased phosphorylation levels of tau protein at the PHF-1 (Ser 396/404) site in the early phase (1–3 h) were observed, suggesting that PI3K is involved in the regulation of phosphorylation of tau protein [35].

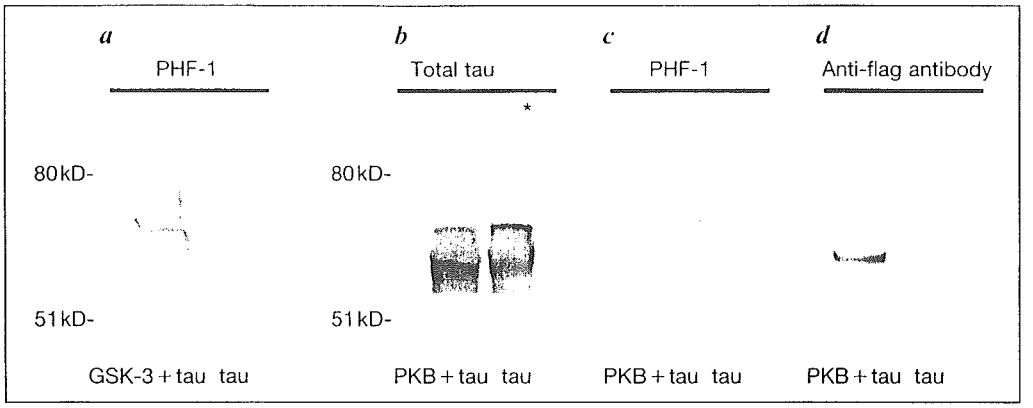

Fig. 5. Phosphorylation of tau protein in 293T cells transfected with tau, GSK-3, and PKB. 293T cells were transfected with tau, GSK-3 and PKB genes. The vectors containing tau (the longest isoform), GSK-3β, and PKBα, were constructed by insertion into pcDNA3.1 (Invitrogen). 293T cells were cotransfected by lipofectamine (Invitrogen) with tau + mock genes, tau + GSK-3 genes, and tau + PKB genes; sufficient expression of gene products was observed 48 h after the transfection. ***a*** The cells were cotransfected with tau + GSK-3 genes and tau + mock genes. The PHF-1 antibody (Ser396/404) revealed more increased phosphorylation of tau protein in cells cotransfected with tau + GSK-3 genes than in cells cotransfected with tau + mock genes (***b–d***) The cells were c-transfected with tau + PKB genes and tau + mock genes. ***b*** Prior to application of the first antibody, membrane was treated with alkaline phosphatase, to observe total tau protein. After treatment, the Tau-1 antibody that reacted with dephosphorylated tau protein at Ser198/199/202 revealed similar expression of tau protein in cells cotransfected with tau + PKB genes and with tau + mock genes. ***c*** The PHF-1 antibody revealed decreased phosphorylation of tau protein in cells co-transfected with tau + PKB genes than in cells co-transfected with tau + mock genes, suggesting that phosphorylation of tau protein by GSK-3 is attenuated by overexpressed PKB. ***d*** Anti-Flag antibody staining was observed only in cells cotransfected with tau + PKB genes, suggesting the PKB gene was appropriately expressed in this experiment.

To confirm the involvement of PKB and GSK-3 in the regulation of phosphorylation of tau protein, 293T cells were transfected with GSK-3 and PKB (fig. 5). The vectors containing tau (the longest isoform), GSK-3β, and PKB-α (generous gifts from M. Goedert, Medical Research Council, UK, A. Takasima, Riken, Japan, and U. Kikkawa, Kobe University, Japan, respectively) were constructed by insertion into pcDNA3.1 (Invitrogen). 293T cells were cotransfected with tau + mock genes, tau + GSK-3 genes, and tau + PKB genes, and sufficient expression of gene products was observed 48 h after the transfection. The PHF-1 antibody (Ser396/404) revealed more increased phosphorylation of tau protein in cells cotransfected with tau + GSK-3 genes than in cells cotransfected with tau + mock genes (fig. 5a). In the membrane treated with alkaline phosphatase, the Tau-1 antibody that reacted with total tau protein revealed a similar expression of tau protein in cells cotransfected with tau + PKB genes,

and with tau + mock genes (fig. 5b). Anti-Flag antibody staining was observed only in cells co-transfected with tau + PKB genes, suggesting the PKB gene is appropriately expressed in this experiment (fig. 5d). Then the PHF-1 antibody revealed decreased phosphorylation of tau protein in cells cotransfected with tau + PKB genes than in cells cotransfected with tau + mock genes, suggesting that phosphorylation of tau protein by GSK-3 is attenuated by overexpressed PKB (fig. 5c). Taken together, the PI3K pathway regulates tau phosphorylation in cultured cells.

Activated Kinases Colocalized with Phosphorylated Tau Protein in AD

As described above, GSK-3 might be a major kinase involved in the formation of abnormally phosphorylated tau protein in AD. Biochemical analysis revealed that the levels of GSK-3, as determined by indirect ELISA, are increased by approximately 50% in the postsynaptosomal supernatant from AD brains as compared with the controls [36]. Immunohistlogical analysis revealed that GSK-3 is prominently present in neuronal cell bodies and their processes and colocalizes with neurofibrillary changes in AD brain [36]. Furthermore, active GSK-3β, phosphorylated at Tyr 216, was found to initially accumulate in the cytoplasm of pretangle neurons [37]. And these active GSK-3-positive neurons appear initially in the pre-alpha layer of the entorhinal cortex and extend to other brain regions, coincident with the sequence of the development of neurofibrillary changes [37]. It was also reported that total GSK-3α, total GSK-3β, and active GSK-3β were found to colocalize with the granulovacuolar degeneration and to be associated with the granules of the granulovacuolar bodies [38]. Further, GSK-3β was expressed in neurons containing neurofibrillary tangles, but only a small proportion of intracellular neurofibrillary tangles was observed to be GSK-3β-immunoreactive [38]. It suggests that neurons developing granulovacuolar degeneration sequester an active form of GSK-3 in this compartment or that activation of GSK-3 is involved predominantly in the early stages of neurodegeneration.

As to the intracellular signal transduction pathway, the upstream regulator of GSK-3 was also investigated in AD brains. As mentioned above, PKB is an important intermediate in the PI3K-signaling cascade that acts to phosphorylate GSK-3β at its serine 9 residue, thereby inactivating it. The amount of activated PKB phosphorylated at Thr308 increased in correlation to the progressive sequence of neurofibrillary changes assessed according to Braak's criteria [39]. This activated PKB was found to appear in particular in neurons that are known to later develop NFTs in AD [39]. Western blotting showed that activated PKB